Is the universe static?

David F. Crawford *

School of Physics**, University of Sydney
Camperdown, NSW, 2006, Australia

June 30, 2021

ABSTRACT

Context. Observations of the light curve widths and peak flux densities of type Ia supernovae are traditional measurements for investigating cosmology. It is shown that a static, tired light, cosmology theory predicts the same redshift dependence of width$\propto (1+z)$, as an expanding cosmology. A completely new analysis of 1,413 type Ia supernovae and 653,338 quasar magnitudes is used to investigate whether a static cosmology is viable.
Aims. The aim is to show that the observations are consistent with a simple model of type Ia supernovae and then to use the measurements of their light curve widths and magnitudes to compare a static cosmology with an expanding cosmology.
Methods. The light curve widths of the type Ia supernovae are determined by the direct fit of the observed flux densities as a function of epoch to a standard template. This provides width and peak magnitude estimates for each supernova. Number density and magnitudes of quasars as a function of redshift provide additional data.
Results. It is shown that the regression equation for the observed widths is $w = (1.043 \pm 0.006) + (0.948 \pm 0.027)z$. The regression of peak absolute magnitude as a function of redshift is $M(z) = -(19.088 \pm 0.012) - (0.124 \pm 0.107)z$. Both regressions are consistent with both cosmologies. The number density and magnitudes of quasars provides additional evidence for a static universe.
Conclusions. Although an expanding universe could be valid, there is strong evidence that the universe is static.

Key words. cosmology: large-scale structure of universe: – supernovae:

1. INTRODUCTION

For many decades the current cosmological paradigm as been that for an expanding universe. The major purpose of this paper is to examine the observation evidence for a static universe and to compare it with an expanding universe.

Nearby type Ia supernovae are well known to have essentially identical light curves that make excellent cosmological probes. The observational evidence for standard time dilation has a long history with notable papers being Goldhaber et al. (2001, 1996) and Blondin et al. (2008). More recent contributions that have used the SALT2 or equivalent methods of analysis are Kowalski et al. (2008); Wood-Vasey et al. (2008); Kessler et al. (2009a); Amanullah et al. (2010); Conley et al. (2011); Betoule et al. (2014); Scolnic et al. (2018). All of these analyses use the SALT2 method to determine the widths and peak flux densities of the supernovae. It is shown in §10 that there is a fundamental problem with SALT2 that it provides a set of parameters that a self consistent with the data but cannot be used to validate the Λ Cold Dark Matter (Λ-CDM) cosmology.

The static model of type Ia supernovae observations used here has two main constituents. The first is that the redshift is due to a simple energy loss that is a function of distance. This has the consequence that the redshift is not proportional to the distance but has a logarithmic dependence shown by Eq. 5. The specific static model used here for numerical comparisons is Curvature Cosmology which is briefly described in the appendix.

The second constituent is that the observed peak flux density is the product of an intrinsic flux density, which is what would be measured by a nearby observer and a cosmological factor due to energy loss during the travel from the supernovae. This is independent of any intrinsic properties of the supernova and only depends on the distance travelled. Thus the intrinsic and cosmological effects are treated as being completely independent.

The results for the type Ia supernovae agree with both models and cannot distinguish between them. However the analysis of the number density of quasars as a function of redshift, and their apparent magnitudes shows strong support for the Curvature Cosmology model. Further analysis of other evidence supports this conclusion.

This paper has eight major parts. The first part in §2 is a theoretical analysis of the effects of a redshift that is produced by a simple energy loss.

The second part in §3 describes the data and how it is analysed to obtain supernovae light curve widths, the peak flux densities, and the peak intrinsic magnitudes.

The regression of the light curve widths as a function of redshift is shown in §4 and they show complete agreement with this static model. They also show complete agreement with the values provided by Scolnic et al. (2018).

The fourth part in §5 covers the estimation of the apparent and absolute flux densities and shows that the apparent magnitudes agree with with the values provided by Scolnic et al. (2018).

* email:davdcraw@gmail.com
** Retired

The fifth part in §6 provides the distance modulus for the static cosmology.

The sixth part in §7 shows that a regression of absolute magnitude verses redshift is consistent with no dependence on redshift which means that the static model is completely consistent with these observations.

The seventh part in §8 provides a measurement of the Phillip's effect which shows that supernovae with wider light curves are also brighter.

The eighth part in §9 provides an analysis of the number density of 653,338 quasar redshifts from the sixteenth Sloan Digital Sky Survey Quasar Catalog. These number densities show strong support for a static cosmology.

The paper concludes with comments on SALT2 and the Λ-CDM cosmology that argues that the results obtained by Scolnic et al. (2018) and others cannot be used to provide support for an expanding universe. It is also argued that it is consistent with the analysis of Thomas Kuhn in that this work requires a new paradigm. It should not be rejected simply because it is inconsistent with the current expansion paradigm.

Since this paper is arguing for a change to the current paradigm of an expanding universe it is a broad brush analysis that omits many minor details such as the effects of host galaxies and gravitational lensing.

Furthermore it is assumed for this analysis that the intrinsic properties of the type Ia supernovae light curves are the same at all redshifts. In other words, there is no evolution. It is also assumed that minor differences in the subtypes of type Ia supernovae and effects of the host galaxy do not have a significant dependence on redshift. Hence their main effect is to increase the background noise.

For convenience it is assumed that the wavelength dependence of a filter can be replaced by a single value ,λ, which is the mean wavelength for that filter.

2. REDSHIFTS AND TIME DILATION

The Hubble redshift law states that distant objects appear, on average, to have an apparent velocity of recession that is proportional to their distance. Since this is consistent with models in General Relativity that have universal expansion, such expanding models have become the standard cosmological paradigm.

Classically, this redshift was obvious because in these models spectral lines are shifted in wavelength exactly like any other time-dependent phenomena.

However quantum mechanics tells us that light is transmitted by photons whose effective wavelength is determined from their momentum by the de Broglie equation $\lambda = hc/E$ where E is their energy and λ is their effective wavelength.

Consequently the Doppler effect and the universal expansion can be explained by an actual loss (or gain) of photon energy. Thus redshifts may be due to any process that causes a loss of photon energy. Because of quantum mechanics, the rigid nexus between the shifts in wavelength of spectral lines and other time variations is broken.

Since cosmology only controls the transmission of the light, it follows that the shape of the received supernovae light-curve must be the same as the shape of the intrinsic light curve but with, possibly, different scale factors. Consequently, all of the cosmological information is contained in the dependence of these scale factors with redshift.

Thus, assuming that all light curves are identical, it is only necessary to measure the two parameters, the peak flux density and the width of the light curve for each supernova, in order to investigate the cosmology of the universe.

If the observed wavelength of a type Ia supernovae at a redshift of z is λ then by definition, the intrinsic (rest frame) wavelength, ϵ, is

$$\epsilon = \lambda/(1+z). \tag{1}$$

The static supernova model requires that observed width of any light curve from a distant object is the product of an intrinsic width (rest frame width), with a cosmological factor due to energy loss. Thus

$$w_{obs}(z,\lambda) = r(z,\lambda) \times w_{int}(\epsilon), \tag{2}$$

where $r(z,\lambda)$ is the width factor due to cosmological energy loss.

For a static universe where the redshift is due to a simple energy loss, an obvious equation for this photon energy loss has the form

$$\frac{1}{E}\frac{dE}{ds} = -\alpha, \tag{3}$$

where s is the distance, E is the photon energy, and α is the relative energy loss rate and it is assumed here that this rate of energy loss is independent of location. Then this equation can be integrated to get

$$s = \ln(E/E_0) \tag{4}$$

where E_0 is the initial energy when $s = 0$ and α is absorbed into s.

If λ is the observed wavelength and ϵ is the emitted wavelength at s_0, then from Eq.1 and since $E \propto 1/\lambda$ we get for the transmission over the distance, s,

$$s = \ln(1+z). \tag{5}$$

Clearly s has the same units as the redshift so that the actual distance, S, is

$$S = c \times \ln(1+z)/H, \tag{6}$$

where c is the velocity of light and H is Hubble's constant. The inverse of this equation is equivalent to a new definition of Hubble's Law, namely

$$z = \exp(HS/c) - 1 \qquad \text{new Hubble's Law}, \tag{7}$$

where S is the distance, and which directly relates the redshift to the distance rather than assuming an effective velocity.

The interesting thing about this equation is that it shows that there is a nonlinear relationship between redshift and distance. Since we do not know the actual distance, s we have to use the redshift as a measure of distance.

From Eq. 5 we get $dz/ds = (1+z)$ which is the ratio of the differential distance at a redshift of z to that at zero redshift. Hence, assuming a constant velocity of transmission we get

$$w(z)/w_0 = 1 + z. \tag{8}$$

Thus in a static universe with the energy loss rate given by Eq. 3 the widths will have the same redshift dependence as in an expanding universe.

3. The analysis of type IA supernovae light curves

3.1. The raw observations

The type Ia supernova data used here comes from the Supernovae Legacy survey (SNSL), the Sloan Digital Survey (SDSS) (both sourced from the SNANA website Kessler et al. (2009b)), and the Panoramic Survey Telescope and Rapid Response System, (Pan-STARRS), supernova survey (Kaiser et al. 2010; Jones et al. 2018; Scolnic et al. 2018) and those observed by the Hubble Space Telescope (HST) (Riess et al. 2007; Jones et al. 2013). The observations of type Ia supernovae from Pan-STARRS, (PS1), were accessed from the site `https://archive.stsci.edu/prepds/ps1cosmo/jones` and the file datatable.html.

In 2018 Pan-STARRS consisted of two 1.8-m Ritchey-Chrétien telescope located at Haleakala in Hawaii and could record almost 1.4 billion pixels per image. It is designed to detect moving or variable objects on a continual basis. An image with a 30 to 60 second duration can record down to an apparent magnitude 22. The whole visible sky will be surveyed four times a month.

3.2. The reference light curve

The essential aim of this analysis is to determine the width of the light curve by examining the raw observations of type Ia supernovae. A critical part in measuring the light curve width of type Ia supernovae light curves is to have a reference light curve. In order to remove any possible bias, a standard independent template, the B band Parab-18 from Table 2 from Goldhaber et al. (2001) which has the first half-peak width at -10.1 days and the second half-peak width at 22.3 days is used. Consequently all widths are relative to this light curve.

3.3. Fitting Each Light Curve

The purpose of the light-curve analysis is to obtain estimates of the peak flux density, the width of the light-curve relative to the template and the epoch offset of the light curve. This offset is a nuisance parameter that allows for the unknown epoch of the peak flux density and is defined to be the epoch difference between the fitted light curve relative to the observed epochs. For convenience define the function $g_i(p_i, q, w)$ by

$$g_i(p_i, q, w) = C((p_i - q)/w), \tag{9}$$

where p_i is the epoch w is the computed width, $C((p_i - q)/w)$ is the reference light curve, and q is the epoch offset. Then the overall log-likelihood function is

$$\mathcal{L} = -\frac{1}{2}\sum_{i=1}^{n}\left[\left(\frac{f_i - Fg_i(p_i, q, w)}{\sigma_i}\right)^2 - \ln(\sqrt{2\pi}\sigma_i)\right] \tag{10}$$

where f_i is the observed flux density for each epoch p_i; σ_i is the flux density uncertainly, and F is the peak flux density. Since the last term in Eq. 10 is irrelevant for all cases used here, it is ignored.

The major problem is to determine the epoch offset q. The search method used was to estimate the average flux density for every daily epoch in the observed range. This averaging used a Gaussian weight factor with the $weight = \exp(-(p_i - p_0)^2)$ where p_i is the epoch of a nearby observation and p_0 is referenced epoch. The search assumed that the width for each supernova was $1 + z$. The day with the largest average flux density defined the initial epoch offset.

Since the width should be the same for all filters, each supernova has a single width.

Next a numerical method (Powell's method Press et al. (2002)) was used to determine the width and epoch offset using Eq. 10. Note that in the likelihood (Eq 10) each flux density and each peak flux density is divided by its uncertainty which means that fitted width is independent of individual filter calibrations and all can be included in the same expression.

At each step of the maximization the peak flux density for each filter was determined for that epoch offset and width by a direct use of the equation

$$F = \sum_{i=1}^{n}(f_i g_i/\sigma_i)/\sum_{i=1}^{n} g_i^2/\sigma_i). \tag{11}$$

A crucial step was to eliminate any observation for which the absolute value of the expression $(f_i - Fg_i)/\sigma_i$ was greater than 9. This was done on the fly so that an expression may be rejected early in the maximization but may be valid once there were better estimates of the parameters.

Finally, the uncertainty in the width was determined from the proposition that the likelihood function, $(\mathcal{L})$ as a function of width is equivalent to the likelihood of a Gaussian function of width with a standard deviation equal to the width uncertainty.

It must be noted that the fitting procedure is completely independent of the redshift and is also independent of the filter type. Although each filter had its own estimate of its peak flux density, the width came from a common fit to all filters.

The final result was an estimate of the width and its uncertainty for the supernovae and estimates of the peak flux density and its uncertainty for each of its filters.

Table1 shows the statistics for the selected supernovae. The selection criteria was that there was a good fit and the width was between 0.6 and 4.0 and the width uncertainly was less than 0.3. From 1,747 initial candidates there 1,422 that satisfied these criteria and also had a good fit. Most of the rejections were because there were insufficient observations prior the peak epoch or that were inconsistencies between different filter flux densities.

4. Observed widths

Since the analysis assumes that the intrinsic width is one,an important result of this width analysis is a regression of $w_{obs}(z)$ as a function of z for all the 1,422 accepted observations which provides

$$w_{obs}(z) = (1.043 \pm 0.006) + (0.948 \pm 0.027)z. \tag{12}$$

The widths for all the supernovae are shown in Figure 1. It is clear that the slope is consistent with the expected dependence of $w(z) = 1 + z$. Thus it is consistent with both expanding and static models.

Scolnic et al. (2018) provides a table of the widths for the Pan-STARRS supernova. For 1,168 type Ia supernovae the regression for the width variable x_1 is

$$x_1^{obs}(z) = -(0.224 \pm 0.030) - (0.074 \pm 0.231)x_1, \tag{13}$$

Table 1. Light-curve numbers for each filter

Filter	λ/μm	N[a]	N[b]
U	0.365	37	0
B	0.445	66	0
V	0.551	66	0
R	0.658	32	0
I	0.809	34	0
u	0.354	126	0
g	0.475	366	970
r	0.622	397	970
i	0.763	397	971
z	0.905	360	970
F775W	0.771	7	0
F850LP	0.907	16	0

[a] Number of supernovae from other catalogues.
[b] Number of supernovae for the ps1 catalogue.

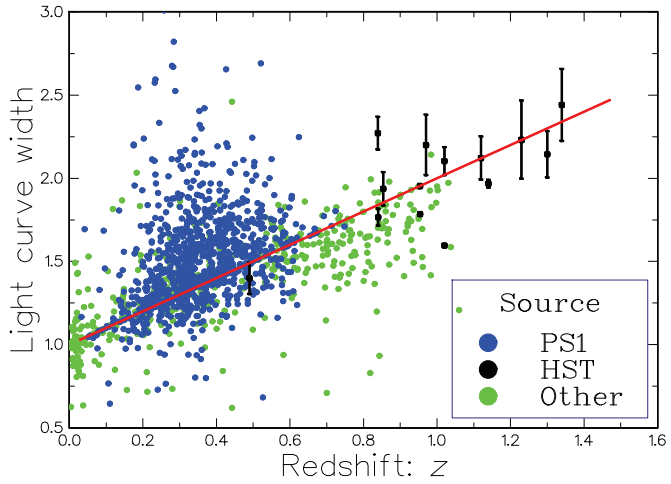

Fig. 1. A plot of the type Ia supernovae light curve observed widths for all the filters. The blue dots are for the PS1 and the black dots with error bars show the HST observations. All other observations are shown by the green dots. The red line shows a $(1+z)$ dependence

where x_1 is a measure of $width/(1+z)-1$. Thus the Scolnic et al. (2018) Pan-STARRS widths are consistent with the $(1+z)$ width dependence.

5. Flux densities and magnitudes

5.1. Malmquist bias

Although the type Ia supernova model has a fixed absolute magnitude, its measurement is subject to the usual uncertainties. This is why they can be observed at large redshifts beyond the nominal limit of the telescope. However most of the observations come from the PS1 survey which is essentially providing a continuous record of the sky so that the simple Malmquist bias is not applicable. And since they provide the majority of the observations there is no attempt to apply a correction for Malmquist bias.

Table 2. Intrinsic magnitude as a function of intrinsic wavelength

ϵ	0.2	0.3	0.4	0.5	0.6	0.7	0.8
Mag.	4.35	1.13	0.03	-0.34	0.21	0.46	0.082

5.2. Intrinsic magnitudes

Since the intrinsic wavelength is defined by $\epsilon = \lambda/(1+z)$, it is clear that there it has a strong dependence on redshift and the intrinsic magnitude is strongly correlated with the cosmology ratio. However all the observations for a particular supernova must have the same cosmological ratio.

For convenience it helps to convert all the flux densities into magnitudes. All observed apparent magnitudes except the those in the SDSS catalogue were calculated by $m_i = 27.5 - 2.5\log_{10}(F_i)$ where F_i is the peak flux density and i is the supernova identifier. Those in the SDSS catalogue used $m_i = 24.5 - 2.5\log_{10}(F_i)$. Since the light curve widths are not relevant to the magnitudes, the peak flux densities were computed using the theoretical width of $w = (1+z)$.

Thus a method of separating the cosmological ratio from the intrinsic magnitude is to use data from supernovae with many filters. Since the cosmological contribution to the flux density is the same for each filter, we can get an estimate of the intrinsic magnitude by subtracting the average magnitude of all the filters for that supernova from the observed magnitude for that filter.

Since nearly all the supernovae had at least four different filter observations the method of determining the average peak flux density was to use general linear least squares method to estimate the observed magnitude for each supernova. This method is identical to simple linear regression except it replaces the variables by vectors and the elements in the vectors are powers of λ. In this case only supernova with at least three filters were select and they were fitted with either a parabolic (when there was only three filters available) or a cubic equation. Then the average magnitude was its value at a common intrinsic wavelength, $\epsilon = 0.445\mu$m (chosen to be the B filter wavelength). The difference between each observed filter magnitude and this reference magnitude provides an estimate if the intrinsic magnitude for each observed wavelength.

Thus for each supernova and each observed wavelength, λ, there is an estimate of its intrinsic magnitude at the intrinsic wavelength, ϵ.

$$\begin{aligned} m_{int} &= (23.9 \pm 1.8) - (162.0 \pm 14.5)\epsilon \\ &\quad +(400.6 \pm 43.4)\epsilon^2 - (431.2 \pm 55.8)\epsilon^3 \\ &\quad +(173.2 \pm 26.1)\epsilon^4, \end{aligned} \tag{14}$$

where the uncertainties are correlated and are the square roots of the diagonal elements of the covariance matrix.

A general linear least squares method as a function of ϵ was used to obtain the fitted function shown in Eq. 14, and the individual intrinsic magnitude data points and Eq. 14 are shown in Figure 2.

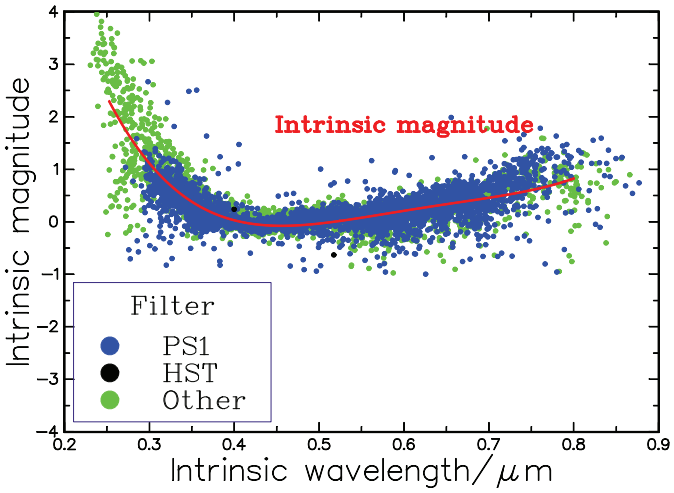

Fig. 2. The intrinsic magnitude of type Ia supernovae as a function of intrinsic wavelength. The red curve shows the general least squares fit to the data points, Eq. 14.

6. Static cosmology

The static model used here is Curvature Cosmology, a summary of it is given in the appendix. Its distance modulus is defined by $\mu(z) = m - M$. This analysis uses the reduced Hubble constant, h=H/(100 kms^{-1} Mpc^{-1}), with the value $h = 0.644$. The constant, $A = 42.384$, is the magnitude at the reference distance of 10 pc, of a source with a flux density of 3,720 Jy.

It is convenient to introduce a variable, $\chi = \ln(1+z)/\sqrt{3}$, then the distance modulus is

$$\mu(z) = 2.5\log_{10}((1+z)[\sqrt{3}\sin(\chi)/h]^2) + A. \quad (15)$$

The apparent magnitude for each supernova and filter is defined to be the observed magnitude minus the intrinsic magnitude defined by Eq. 14. This apparent magnitude is shown in Figure 3. The red curve shows the distance modulus for the static cosmology.

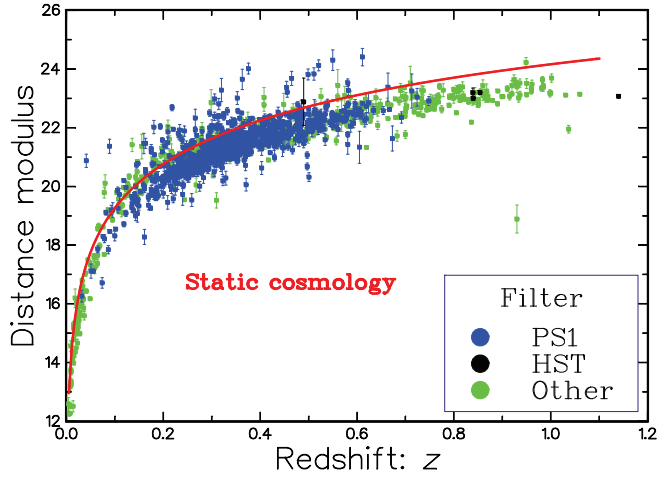

Fig. 3. The cosmological apparent magnitude of type Ia supernovae as a function of redshift. The red curve shows the static distance modulus a function of redshift.

Scolnic et al. (2018) also provides a table of the peak flux density for the Pan-STARRS supernova. For 1,168 type Ia supernovae the regression for these peak flux density as a function of the observed static flux densities is

$$m_{ps1} = (0.557 \pm 0.005) + (0.997 \pm 0.027)m_{obs}, \quad (16)$$

with a correlation coefficient of 0.971. Thus there is excellent agreement between the two peak flux density estimates.

7. Absolute magnitude

The next step is to compute the peak absolute magnitudes and compare their dependence on redshift. The dependence of the peak absolute magnitudes on distance is shown in Eq. 17 and in Figure 4.

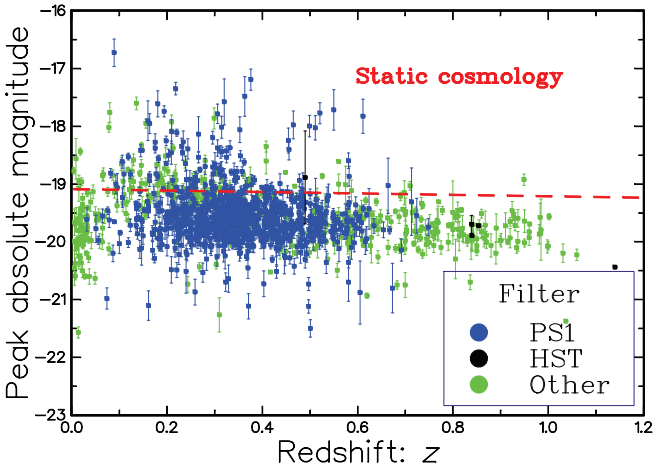

Fig. 4. The absolute magnitude of type Ia supernovae as a function of distance for the static cosmology. The blue curve shows the regression equation of the absolute magnitude as a function of redshift.

Since the intercept is a free parameter, it is the slope of the regression that provides an estimate of the correction needed to make the cosmology agree with the data. The regression for 1.413 absolute magnitudes of type Ia supernovae as a function of redshift is

$$M(z) = -(19.088 \pm 0.012) - (0.124 \pm 0.107)z \quad (17)$$

Since -0.127 ± 0.107 is statistically identical to zero the absolute magnitude is consistent with both expanding and static models.

8. Phillip's effect

A regression of the absolute magnitudes for the static model versus the widths (divided by $(1+z)$) is $(-19.79 \pm 0.04) - (0.52 \pm 0.22)w$. This value is significant and shows that supernovae with wider light curves are also brighter.

9. Quasars

Another way to compare cosmologies is to examine the number density of quasars. All quasar data used here is taken from the Sloan Digital Sky Survey Quasar Catalog: Sixteenth Data Release (DR16Q) Lyke et al. (2020). Since the majority of these objects gave been discovered by a flux density limited survey without knowledge of the redshift the observed number density should provide a reasonable guide the number density distribution of the observed cosmology.

Figure 5 shows the number density for 653,338 quasars as a function of redshift. The black line is the observed number in a uniform distribution covering a range of redshift from zero to 7.0 over 100 values. The rapid fall of the observed density at larger redshifts is a consequence of the scarcity of high redshift quasars and the statistical distribution of the quasar flux densities selection.

The blue line in Figure 5 shows the expected distribution for Curvature Cosmology. Its slow decrease with larger redshifts is partly because the expected density should be a constant as a function of distance and its relationship to redshift is $s = \ln(1+z)$, Eq.5. The red line shows the expected distribution for the Λ-CDM cosmology with $\Omega_m = 0.309$ and $w = -1$. Both curves were normalised to have 10044 quasars in box 10, with a redshift of 0.623.

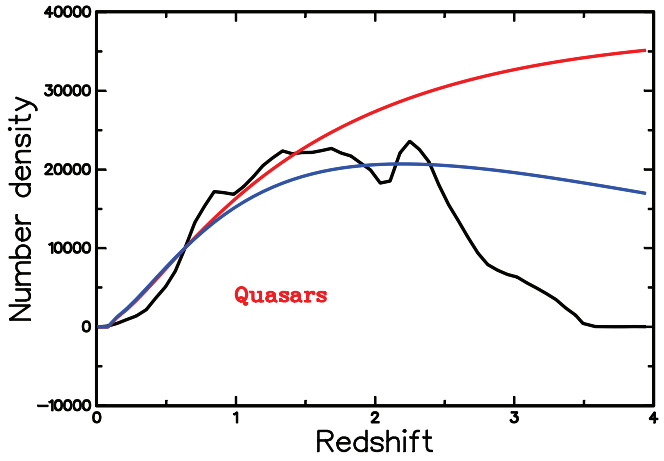

Fig. 5. The number density of 653,338 quasars as a function of redshift. The blue line shows the expected distribution for the Curvature Cosmology and the red line for shows the expected distribution for the Λ-CDM cosmology.

Figure 5 shows a stronger agreement with the Curvature Cosmology than for the Λ-CDM cosmology. The red curve shows a much faster increase of density with redshift that is due to universal expansion.

The observed quasar apparent magnitudes are the sum of an intrinsic magnitude and a cosmological magnitude, that is

$$m_{cos}(z) = m_{obs}(z,\lambda) - m_{int}(\epsilon). \quad (18)$$

Table 3. rms of the absolute quasar magnitude for the models

Model	Number	rms
Euclidean	653,338	1.2277
Λ-CDM	653,338	1.4293
Curvature Cosmology	653,338	1.1856

Without out making any assumptions about the intrinsic properties of the quasars it is clear that the rms (root mean square) of the absolute magnitude will be the smallest for the best fitting cosmology. The calculation of the rms was done using the distance moduli for the Λ-CDM model, the Curvature Cosmology and a Euclidean model. The distance modulus for the Euclidean model is (cf. Eq.5)

$$\mu(z) = 2.5[\log_{10}((1+z)(\ln(1+z)/h)^2] + A. \quad (19)$$

All these rms values are highly significant and show that Curvature Cosmology has the best fit.

10. Comments on expansion cosmology

Since this paper challenges the expanding universe paradigm some comments on the current Λ-CDM cosmology are necessary. Currently most analyses (see list in the introduction) use the SALT2 (Guy et al. 2010, 2007) procedure to determine the light curve width and peak flux density of type Ia supernovae. The ingenious part of this analysis is that it overcomes the problem of a sparse coverage of intrinsic magnitudes. An observed magnitude $m_{obs}(z,\lambda)$ requires an estimate of the intrinsic magnitude $m_{int}(\epsilon)$ in order to obtaining the cosmological magnitude $m_{cos}(z)$ (Eq. 18).

Since $\epsilon = \lambda/(1+z)$ the intrinsic magnitude must be the same as that for a different redshift, $z^* = \lambda/\epsilon - 1$. Thus by using a common set of intrinsics magnitudes it is possible to obtain a self consistent set of magnitudes. However this means using the same cosmological magnitudes to determine the intrinsic magnitudes which looses one degree of freedom and it is a circular procedure that makes all the magnitude estimates interdependent. For example adding a constant to all the observed magnitudes would change the estimated intrinsic magnitudes that, to the first order, would cancel the change and leave the cosmological magnitude unchanged. The actual SALT2 calibration process is more complex than this simple description in that it does not separate the two types of magnitudes but uses color differences based on filter wavelengths. Nevertheless its use to calibrate supernovae magnitudes is suspect.

The Λ-CDM cosmology distance modulus has six parameters that are mainly determined from the type Ia supernovae observations. Because these magnitudes are used to find the values of these parameters they cannot then be used to validate this cosmology.

11. CONCLUSIONS

It has been shown that the light curve widths and their peak magnitudes are consistent with a static model. However previous analyses listed in the introduction show considerable support for the Λ-CDM cosmology. Thus the observational data for the type Ia supernovae presented here is

equally supportive of both cosmologies. However the analysis of the number density of quasars as a function of redshift, and their apparent magnitudes, shows strong support for the Curvature Cosmology model.

The final step is to consider other factors that could influence the decision on which model provides the best description of the universe.

It is argued above that the use of type Ia supernovae light curves cannot be used to validate Λ-CDM cosmology. If we omit type Ia supernovae observations the Λ-CDM cosmology is poorly supported by direct observations. Furthermore it has many unresolved problems such as inflation, dark matter and dark energy. Since none of these properties are substantiated by other external observations they do not provide any support for this cosmology. Consequently there is only poor observational evidence to support the Λ-CDM cosmology.

The major argument against Curvature Cosmology is that it is based on two new hypothesises that are not yet validated. However it does have other observations that provide support.

A major one is that it can explain the X-ray background radiation. The X-rays come from a very hot intergalactic plasma with a temperature of $(2.64 \pm 0.04) \times 10^9$ K. The plasma has a density $N = 1.55 \pm 0.01$ hydrogen atoms per cubic meter. The Curvature Cosmology model has only one free parameter which is the value of this density.

With this density it predicts a Hubble constant of 64.4 kms^{-1} $(Mpc)^{-1}$. It also predicts the Cosmic Microwave Background radiation with a temperature of 3.18K.

It is consistent with Tolman surface brightness observations, angular size observations and quasar variability and it could possibly explain galaxy rotation curves.

In a stationary universe material will be recycled between galaxies and the intergalactic medium which has a large enough temperature to provide nuclear reactions.

Finally the hypothesis of Curvature Pressure will prevent the final collapse of an object to form a black hole and provide an extremely compact object with most of the external properties of a black hole. Moreover it could be the cause a large galactic and stellar jets.

In his book, "The Structure of Scientific Revolutions", (Kuhn 1970) Thomas Kuhn argues that the development of a science is not uniform but has alternating 'normal' and 'revolutionary' (or 'extraordinary') phases. The revolutionary phases are not merely periods of accelerated progress, but differ qualitatively from normal science. Normal science does resemble the standard cumulative picture of scientific progress, on the surface at least.

I believe that this paper is in this "revolutionary" class and should not be arbitrarily dismissed because it disagrees with the current paradigm.

The final conclusion is that the Curvature Cosmology is valid and the universe is static

Acknowledgement

This research has made use of the NASA/IPAC Extragalactic Database (NED) that is operated by the Jet Propulsion Laboratory, California Institute of Technology, under contract with the National Aeronautics and Space Administration. The calculations have used Ubuntu Linux and the graphics have used the DISLIN plotting library provided by the Max-Plank-Institute in Lindau. None.

References

Amanullah, R., Lidman, C., Rubin, D., et al. 2010, ApJ, 716, 712
Betoule, M., Kessler, R., Guy, J., et al. 2014, A&A, 568, A22
Blondin, S., Davis, T. M., Krisciunas, K., et al. 2008, ApJ, 682, 724
Braginskij, V. B., & Panov, V. I. 1971, Uspekhi Fizicheskikh Nauk, 105, 779
Conley, A., Guy, J., Sullivan, M., et al. 2011, ApJS, 192, 1
Crawford, D. F. 1987a, Australian Journal of Physics, 40, 459
—. 1987b, Australian Journal of Physics, 40, 449
—. 1991, ApJ, 377, 1
—. 1993, ApJ, 410, 488
—. 1995a, ApJ, 440, 466
—. 1995b, ApJ, 441, 488
—. 1999, Australian Journal of Physics, 52, 753
—. 2006, Curvature Cosmology (BrownWalker Press)
—. 2009a, ArXiv e-prints, arXiv:0901.4169
—. 2009b, ArXiv e-prints, arXiv:0901.4172
Dicke, R. H. 1964, Nature, 202, 432
Ellis, G. F. R. 1984, Annual Review of Astronomy and Astrophysics, 22, 157
Eötvös, R. V., Pekár, D., & Fekete, E. 1922, Annalen der Physik, 373, 11
Giacconi, R., Gursky, H., Paolini, F. R., & Rossi, B. B. 1962, Phys. Rev. Lett., 9, 439
Goldhaber, G., Boyle, B., Bunclark, P., et al. 1996, Nuclear Physics B Proceedings Supplements, Vol. 51, 51, 123
Goldhaber, G., Groom, D. E., Kim, A., et al. 2001, ApJ, 558, 359
Guy, J., Astier, P., Baumont, S., et al. 2007, A&A, 466, 11
Guy, J., Sullivan, M., Conley, A., et al. 2010, A&A, 523, A7
Jones, D., Scolnic, D., Riess, A., et al. 2018, in American Astronomical Society Meeting Abstracts #231, Vol. 231, 308.06
Jones, D. O., Rodney, S. A., Riess, A. G., et al. 2013, ApJ, 768, 166
Kaiser, N., Burgett, W., Chambers, K., et al. 2010, in Ground-based and Airborne Telescopes III, Vol. 7733, 77330E
Kessler, R., Becker, A. C., Cinabro, D., et al. 2009a, ApJS, 185, 32
Kessler, R., Bernstein, J. P., Cinabro, D., et al. 2009b, PASP, 121, 1028
Kowalski, M., Rubin, D., Aldering, G., et al. 2008, ApJ, 686, 749
Kuhn, T. S. 1970, The structure of scientific revolutions
Lyke, B. W., Higley, A. N., McLane, J. N., et al. 2020, ApJS, 250, 8
Mather, J. C., Cheng, E. S., Eplee, R. E., J., et al. 1990, ApJ, 354, L37
Misner, C. W., Thorne, K. S., & Wheeler, J. A. 1973, Gravitation
Press, W. H., Teukolsky, S. A., Vetterling, W. T., & Flannery, B. P. 2002, Numerical recipes in C++ : The art of Scientific Computing (Cambridge University Press)
Riess, A. G., Strolger, L.-G., Casertano, S., et al. 2007, ApJ, 659, 98
Scolnic, D. M., Jones, D. O., Rest, A., et al. 2018, ApJ, 859, 101
Tolman, R. C. 1934, Relativity, Thermodynamics, and Cosmology
Wood-Vasey, W. M., Friedman, A. S., Bloom, J. S., et al. 2008, ApJ, 689, 377
Zwicky, F. 1937, ApJ, 86, 217

Appendix A: CURVATURE COSMOLOGY

This appendix is provided as a reference and is not used in the main paper. Curvature Cosmology (Crawford 1987b,a, 1991, 1993, 1995a,b, 1999, 2006, 2009b,a) is a complete cosmology for a static universe that shows excellent agreement with all major cosmological observations without needing dark matter or dark energy.(Note that (`http://arxiv.org/abs/1009.0953`) is an update with corrections of the previous work.) This cosmology depends on the hypotheses of Curvature Redshift and Curvature Pressure described below. The basic cosmological model is one in which the cosmic plasma dominates the mass distribution and hence the curvature of space-time. In this first-order model, the effects of galaxies and stars are neglected. The geometry of this cosmology is that of a three-dimensional surface of a four-dimensional hyper-sphere. It is identical to that for Einstein's static universe. For a static universe, there is no ambiguity in the definition of distances and times. One can use a cosmic time and define distances in light travel times or any other convenient measure. Curvature Cosmology obeys the perfect cosmological principle of being statistically the same at all places and at all times.

Appendix A.1: Curvature Redshift

The derivation of Curvature Redshift is based on the fundamental hypothesis of Einstein's general theory of relativity that space-time is curved. As a consequence, for positive curvature, the trajectories of initially parallel point particles, geodesics, will move closer to each other as time increases. Consequently the cross-sectional area of a bundle of geodesics will slowly decrease. In applying this idea to photons, we assume that a photon is described in quantum mechanics as a localized wave where the geodesics correspond to the rays of the wave. Note that this wave is quite separate from an electromagnetic wave that corresponds to the effects of many photons. It is fundamental to the hypothesis that we can consider the motion in space-time of individual photons. Because the curvature of space-time causes the focussing of a bundle of geodesics, this focussing also applies to the wave. As the photon progresses, the cross-sectional area of the wave associated with it will decrease. However, in quantum mechanics, properties such as angular momentum are computed by an integration of a radial coordinate over the volume of the wave. If the cross-sectional area of the wave decreases, then the angular momentum will also decrease. However, the angular momentum of a photon is a quantized parameter that has a fixed value. The solution to this dilemma is that the photon splits into two very low-energy photons and a third that has the same direction as the original photon and nearly all the energy. It is convenient to consider the interaction as a primary photon losing a small amount of energy to two secondary photons. This energy loss will be perceived as a small decrease in frequency. By symmetry the two secondary photons with identical energies are emitted at right angles to the trajectory, which means that there is no angular scattering. Since in quantum mechanics electrons and other particles are considered as waves, a similar process will also apply. It is argued that electrons will interact with curved space-time to lose energy by the emission of very low-energy photons. From (`http://arxiv.org/abs/1009.0953`) we get the basic equation for the fractional change in energy of the photon. This is based on the equation of geodesic deviation (Misner et al. 1973).

$$\frac{1}{E}\frac{dE}{ds} = -\left(\frac{8\pi G\rho}{c^2}\right)^{1/2} = -1.366\times10^{-13}\sqrt{\rho}\,\mathrm{m}^{-1}. \quad (A.1)$$

For many astrophysical types of plasma, it is useful to measure density by the equivalent number of hydrogen atoms per cubic meter: that is we can put $\rho = \mathrm{N}\,\mathrm{M}_H$ and get

$$\frac{1}{E}\frac{dE}{ds} = -3.339\sqrt{N}\,\mathrm{m}^{-1}. \quad (A.2)$$

Thus the rate of energy loss per distance travelled depends only on the square root of the density of the material, which may consist of gas, plasma, or dust. For many astrophysical plasmas the frequency of the emitted photons will be less than the plasma frequency and they will be absorbed and heat the plasma. Another important factor is that if there is any other competing interaction which occurs before the secondary photons are produced it will inhibit the Curvature Redshift. Such an interaction is the coherent multiple scattering that produces refractive index. This can be important for ground bases experiments and for radio frequency observations in the Galaxy. For example, low frequency radio observations in our galaxy will be unaffected by Curvature Redshift.

Appendix A.2: Curvature Pressure

The hypothesis of Curvature Pressure is that for moving particles there is a pressure generated that acts back on the matter that causes the curved space-time. In this case, Curvature Pressure acts on the matter that is producing curved space-time in such a way as to try to decrease the curvature. In other words, the plasma produces curved space-time through its density entering the stress-energy tensor in Einstein's field equations and the action of the velocities of the plasma particles is to try and decrease this curvature.. A simple cosmological model using Newtonian physics illustrates some of the basic physics subsequently used to derive the features of Curvature Pressure. The model assumes that the universe is composed of gas confined to the three-dimensional surface of a four-dimensional hypersphere. Since the visualization of four dimensions is difficult let us suppress one of the normal dimensions and consider the gas to occupy the two-dimensional surface of a normal sphere. From Gauss's law (i.e. the gravitational effect of a spherical distribution of particles with radial symmetry is identical to that of a point mass, at the center of symmetry, equal in value to the total mass.) the gravitational acceleration at the radius r of the surface is normal to the surface, directed inward and it has the magnitude $\ddot{r} = -GM/r^2$ where M is the total mass of the particles and the dots denote a time derivative. For equilibrium, and assuming all the particles have the same mass and velocity we can equate the radial acceleration to the gravitational acceleration and get the simple equation from celestial mechanics of

$$v^2 = \frac{GM}{r}. \quad (A.3)$$

The effect of this balancing of the accelerations against the gravitational potential is seen within the shell as a Curvature Pressure that is a direct consequence of the geometric constraint of confining the particles to a shell. If the

radius r decreases then there is an increase in this Curvature Pressure that attempts to increase the surface area by increasing the radius. For a small change in radius in a quasi-equilibrium process where the particle velocities do not change the work done by this Curvature Pressure (two dimensions) with an incremental increase of area dA is $p_c dA$ and this must equal the gravitational force times the change in distance to give

$$p_c dA = \frac{GM^2}{r^2}\, dr, \tag{A.4}$$

where $M = \sum m_i$ with the sum going over all the particles. Therefore, using Eq. A.3) we can rewrite the previous equation in terms of the velocities as

$$p_c dA = \frac{M\left\langle v^2\right\rangle}{r}\, dr. \tag{A.5}$$

Now $dA/dr = 2A/r$, hence the two-dimensional Curvature Pressure is

$$p_c = \frac{M\left\langle v^2\right\rangle}{2A}. \tag{A.6}$$

Thus in this two-dimensional model the Curvature Pressure is like the average kinetic energy per unit area. This simple Newtonian model provides a guide as to what the Curvature Pressure would be in the General Relativistic model. The extension to different particle masses and velocities uses the basic property of General Relativity that gravitation is an acceleration and not a force. This is supported by Eötvös, Pekár, & Fekete (1922), Dicke (1964), and Braginskij & Panov (1971) who have shown that the passive gravitational mass is equal to the inertial mass to about one part in 10^{12}. The usual interpretation of this agreement is that they are fundamentally the same thing. However, an alternative viewpoint is that the basic equation is wrong and that the passive gravitational mass and the inertial mass should not appear in Newton's gravitational equation. Consequently Newton's gravitational equation is an equation of accelerations and not of forces. The equation for Curvature Pressure in a 3 dimensional high temperature plasma is

$$p_c = \frac{1}{3}\left\langle \gamma^2 - 1\right\rangle \rho c^2, \tag{A.7}$$

where γ is the Lorentz factor, $\langle\rangle$ denotes an average and the 3 replaces the 2 in Eq. A.6 in order to allow for three dimensions. In effect, my hypothesis is that the cosmological model must include this Curvature Pressure as well as thermodynamic pressure. Note that although this has a similar form to thermodynamic pressure it is quite different. In particular, it is proportional to an average over the squared velocities and the thermodynamic pressure is proportional to an average over the kinetic energies. This means that, for plasma with free electrons and approximate thermodynamic equilibrium, the electrons will dominate the average due to their much larger velocities. Including Curvature Pressure into the Friedmann equations provides stable static cosmological model. Including Curvature Pressure from Eq. A.7 the modified Friedmann equations are

$$\begin{aligned} \ddot{R} &= -\frac{4\pi G\rho}{3}\left[1 - \left\langle \gamma^2 - 1\right\rangle\right] R, \\ \dot{R}^2 &= \frac{8\pi G\rho}{3} R^2 - c^2. \end{aligned}$$

Clearly, there is a static solution if $< \gamma^2 - 1 >= 1$, in which case $\ddot{R} = 0$. The second equation, with $\dot{R} = 0$ provides the radius of the universe which is given by

$$R = \sqrt{\frac{3c^2}{8\pi G\rho}} = \sqrt{\frac{3c^2}{8\pi G M_{\rm H} N}}. \tag{A.8}$$

Thus, the model is a static cosmology with positive curvature. Although the geometry is similar to the original Einstein static model, this cosmology differs in that it is stable. The basic instability of the static Einstein model is well known (Tolman 1934; Ellis 1984). On the other hand, the stability of Curvature Cosmology is shown by considering a perturbation ΔR, about the equilibrium position. Then the perturbation equation is

$$\Delta\ddot{R} \propto -\left(\frac{d\langle\gamma^2 - 1\rangle}{dR}\right)\Delta R. \tag{A.9}$$

For any realistic equation of state for the cosmic plasma, the average velocity will decrease as R increases. Thus the right-hand side is negative, showing that the result of a small perturbation is for the universe return to its equilibrium position. Thus, Curvature Cosmology is intrinsically stable. Of theoretical interest is that Eq. A.9 predicts that oscillations could occur about the equilibrium position. Curvature Cosmology has only one free parameter which is taken to be the average cosmic density of $N = 1.55$ hydrogen atoms m^{-3}.

Appendix A.3: X-ray Background Radiation

Since Giacconi et al. (1962) observed the X-ray background, there have been many suggestions made to explain its characteristics. Although much of the unresolved X-ray emission comes from active galaxies, there is a part of the spectrum between about 10 keV and 1 MeV that is not adequately explained by emission from discrete sources. Curvature Cosmology can explain the X-ray emission in the energy range from about 10 keV to 300 keV as coming from a very hot intergalactic plasma. A simple model has a mixture of hydrogen with 8% helium and a density of $N = 1.55 \pm 0.01$ hydrogen atoms per cubic meter or $2.57\times10^{-27}\,\mathrm{kg\,m^{-3}}$. For this density the theoretical temperature is $2.56 \times 10^9\,\mathrm{K}$ for the cosmic plasma. The temperature estimated from fitting the X-ray data is $(2.62 \pm 0.04) \times 10^9\,\mathrm{K}$ which is a good fit. Although this is similar to early explanations of the X-ray emission, it differs in that it depends on the current plasma density. The earlier explanations required the X-ray emission to come from a plasma with about three times that density which conflicts with other observations.

Appendix A.4: Nuclear Abundances

One of the successes of the standard model is in its explanation of the primordial abundances of the light elements. In Curvature Cosmology, the primordial abundance refers to the abundance in the cosmic plasma from which the galaxies are formed. The first point to note is that the predicted temperature of the cosmic plasma is 2.56×10^9 K at which temperature nuclear reactions can proceed. It is postulated that there is a continuous recycling of material from the cosmic gas to galaxies and stars and then back to the gas. Because of the high temperature, nuclear reactions will take

place whereby the more complex nuclei are broken down to hydrogen, deuterium, and helium.

Appendix A.5: Cosmic Microwave Background Radiation

The Cosmic microwave background radiation (CMBR) is produced by very high energy electrons via Curvature Redshift radiation in the cosmic plasma. With $N = 1.55$ the predicted temperature of the CMBR is 3.18 K to be compared with an observed value of 2.725 K (Mather et al. 1990). This prediction does depend on the nuclei mix in the cosmic plasma and could vary from this value by several tenths of a degree. Although the CMBR photons are subject to continuous Curvature Redshift they will be quantized, and since all energy levels are freely available, the black body (Plank function) is their thermal equilibrium spectrum. Differences in the local environment, especially high density, lower temperature, gas clouds, will decrease the flux density of the CMBR and could explain some of the observed spatial fluctuations in the CMBR.

Appendix A.6: No Dark matter

In 1937 Zwicky (1937) found in an analysis of the Coma cluster of galaxies that the ratio of total mass obtained by using the virial theorem to the total luminosity was 500 whereas the expected ratio was 3. The virial theorem is a statistical theorem that states that for an inverse square law the average kinetic energy of a bound system is equal to half the potential energy. This huge discrepancy was the start of the concept of dark matter. It is surprising that in more than eight decades since that time there is no direct evidence for dark matter. Similarly the concept of dark energy (some prefer quintessence) has been introduced to explain discrepancies in the observations of type 1a supernovae. X-ray observations show that the Coma cluster has a large plasma cloud in its center. The Curvature Cosmology model is that the galactic velocity dispersion in the cluster is entirely due to Curvature Redshift of photons passing through the central plasma cloud. For 583 galaxies the rms (root-mean-square) velocity was 893 $\mathrm{km\,s^{-1}}$ and the computed theoretical value was 554 $\mathrm{km\,s^{-1}}$. Considering that it was assumed that both the galaxy distribution and plasma distribution had a very simple geometry this shows that Curvature Cosmology can explain the velocity dispersion in the Coma cluster and Coma cluster observations show no support for dark matter.

Appendix A.7: Galactic rotation

One of the most puzzling questions in astronomy is: why the observed velocity of rotation in spiral galaxies does not go to zero towards the edge of the galaxy. Simple Keplerian mechanics suggest that there should be a rapid rise to a maximum and then a decrease in velocity that is inversely proportional to the square root of the radius once nearly all the mass has been passed. Although the details vary between galaxies, the observations typically show a rapid rise and then an essentially constant tangential velocity as a function of radius out to distances where the velocity cannot be measured due to lack of material. The standard explanation is that this is due to the gravitational attraction of a halo of dark matter that extends well beyond the galaxy. Observations show that our own Galaxy and other spiral galaxies have a gas halo that is larger than the main concentration of stars. It is clear that if the observed redshifts are due to Curvature Redshift acting within this halo, the halo must be asymmetric; otherwise, it could not produce the asymmetric rotation curve. Now the observed velocities in the flat part of the curves are typically 100 to 200 $\mathrm{km\ s^{-1}}$. For realistic values of the densities and sizes of the halo, the predicted velocity is about 163 $\mathrm{km\,s^{-1}}$. Thus, the magnitude is feasible. Although there could be a natural asymmetry in a particular galaxy, the fact that the flattened rotation curve is seen for most spiral galaxies suggests that there is a common cause for the asymmetry. One possibility is that the asymmetry could arise from ram pressure due to the galaxy moving through the intergalactic medium. Although the explanation for galactic rotation observations is limited, it is not excluded.

Appendix A.8: No Black Holes

A theory of Curvature Pressure in a very dense medium where quantum mechanics dominate and where general relativity may be required is needed to develop this model. Nevertheless it is clear that Curvature Pressure would resist a hot compact object from collapsing to a black hole. Because of the potential energy released during collapse, it is extremely unlikely for a cold object to stay cold long enough to overcome the Curvature Pressure and collapse to a black hole. What is expected is that the final stage of gravitational collapse is a very dense object, larger than a black hole but smaller than a neutron star. This compact object would have most of the characteristics of black holes. Such objects could have large masses and be surrounded by accretion discs. Thus, many of the observations that are thought to show the presence of a black hole could equally show the presence of these compact objects. If the compact object is rotating there is the tantalizing idea that Curvature Pressure may produce the emission of material in two jets along the spin axis. This could be the "jet engine" that produces the astrophysical jets seen in stellar-like objects and in many huge radio sources. Furthermore this could be a mechanism to return material to the cosmic plasma. Currently there are no accepted models for the origin of these jets.

Appendix A.9: Olber's Paradox

In Curvature Cosmology Olber's Paradox is not a problem. Visible light from distant galaxies is shifted into the infrared where it is no longer seen and the energy is eventually absorbed back into the cosmic plasma. Everything is recycled. The plasma radiates energy into the microwave background radiation and into X-rays. The galaxies develop from the cosmic plasma, stars are formed which pass through their normal evolution. Eventually all their material is returned to the cosmic plasma.

Appendix A.10: Basic equations for Curvature Cosmology

The geometry is that of a three-dimensional surface of a four-dimensional hyper sphere. For this geometry the radius is $r = R\chi$ where

$$\chi = \ln(1+z)/\sqrt{3}. \tag{A.10}$$

(NB. work prior to 2009 has $\chi = \ln(1+z)/\sqrt{2})$)
The area is

$$A(r) = 4\pi R^2 \sin^2(\chi). \quad \text{(A.11)}$$

The surface is finite and χ can vary from 0 to π. The volume within a redshift z is given by

$$V(z) = 2\pi R^3 \left[\chi - \frac{1}{2}\sin(2\chi)\right]. \quad \text{(A.12)}$$

Using the density $N = 1.55\,m^{-3}$) the Hubble constant is predicted to be

$$\begin{aligned} H &= -\frac{c}{E}\frac{dE}{ds} = (8\pi G M_{\rm H} N)^{\frac{1}{2}} \\ &= 51.69 N^{\frac{1}{2}}\ \text{kms}^{-1}\ \text{Mpc}^{-1} \quad \text{(A.13)} \\ &= 64.4 \pm 0.2\ \text{kms}^{-1}\ \text{Mpc}^{-1}. \end{aligned}$$

The only other result required here is the equation for the distance modulus ($\mu = m - M$), which is

$$\mu = 5\log_{10}[(\sqrt{3}\sin(\chi))/h] + 2.5\log_{10}(1+z) + 42.384. \quad \text{(A.14)}$$

where h=H/(100 $\text{kms}^{-1}\ \text{Mpc}^{-1}$).

Appendix A.11: Basic Results for Curvature Cosmology

Since the ramifications of a static universe are quite profound, a list of the major consequences of Curvature Cosmology is given here. All the numerical results are derived using the cosmic plasma density $N = 1.55$ H atoms m^{-3}.

1. It obeys the perfect cosmological principle.
2. It is stable.
3. There is no dark matter.
4. There is no dark energy. Meaningless.
5. There is no inflation. Meaningless.
6. There is no horizon problem. Meaningless.
7. The cosmic plasma has a density N= $1.55 \pm 0.01\,\text{M}_H\,m^{-3}$).
8. The cosmic plasma has a temperature of $(2.64 \pm 0.04) \times 10^9$ K.
9. The Hubble constant is $64.4\ \text{kms}^{-1}\ (Mpc)^{-1}$.
10. It is consistent with type Ia supernovae observations.
11. It is consistent with GRB observations.
12. It is consistent with quasar luminosity observations.
13. It is consistent with galaxy luminosity observations.
14. It is consistent with Tolman surface brightness observations.
15. It is consistent with radio source counts.
16. It is consistent with quasar variability
17. It is consistent with angular size observations.
18. It is can explain the Cosmic Microwave Background Radiation.
19. The CMBR radiation has temperature of 3.18 K.
20. It can provide a partial explanation for fluctuations in CMBR.
21. It can provide a partial explanation for galactic rotation curves.
22. It can explain the X-ray background radiation.
23. It can possibly explain the cosmic nuclear abundances.
24. Curvature redshift can be investigated with laboratory measurements.
25. There are no black holes but similar objects with a finite size.
26. Universal radius: 3.11×10^{26} m or 1.008×10^{10} pc.
27. Volume: 8.95×10^{80} m^3 or 2.02×10^{31} pc^3.
28. Mass: 2.54×10^{54} kg or $1.28 \times 10^{23} M_{sun}$.